



Eurasia Specialized Veterinary Publication

Entomology Letters

ISSN:3062-3588

2023, Volume 3, Issue 1, Page No: 18-27

Copyright CC BY-NC-SA 4.0

Available online at: [www.esvpub.com/](http://www.esvpub.com/)

## Differences in Gut Microbiota of Healthy and Tiger Band Disease-Infected Oak Tasar Silkworms (*Antheraea proylei* J.)

Yumnam Rajlakshmi Devi<sup>1,2</sup>, Deepak Singh Lourebam<sup>3</sup>, Rahul Modak<sup>2</sup>, Tourangbam Shantibala<sup>4</sup>, Sinam Subharani<sup>5</sup>, Yallappa Rajashekar<sup>1\*</sup>

<sup>1</sup>Insect Resources Laboratory, Animal Resources Programme, Institute of Bioresources and Sustainable Development, IBSD, Takyelpat, Manipur, India.

<sup>2</sup>School of Biotechnology, Kalinga Institute of Industrial Technology, Deemed to be University, Bhubaneswar, Odisha, India.

<sup>3</sup>Department of Pathology, Regional Institute of Medical Sciences (RIMS) Manipur, India.

<sup>4</sup>College of Agriculture and Forestry, CHF, Central Agricultural University, Pasighat.

<sup>5</sup>Regional Sericultural Research Station, Imphal, India.

\*E-mail ✉ [rajacftri77@gmail.com](mailto:rajacftri77@gmail.com)

### ABSTRACT

*Antheraea proylei* J., a vital silkworm species from the Northeastern region of India, is primarily farmed for tasar silk production. This silkworm is highly susceptible to various pathogens, including viruses, bacteria, and fungi, with the recent emergence of the tiger band disease, a viral infection that severely affects larval development and cocoon production, leading to substantial economic losses in the silk industry. The gut microbiota plays a key role in the silkworm's nutrition and immune defense against pathogens. However, there is limited information on the diversity and ecological aspects of the gut microbiota in this tasar silkworm. In this study, we focus on the molecular profiling and histopathological analysis of the gut bacteria in both diseased and healthy silkworms. We observed significant pathological changes in diseased silkworms, including the loss of lumen distortion, turbidity, and a reduction in the secretory layer. In addition, the body fat in the infected silkworms was vacuolated and softened compared to the healthy ones. 16S rRNA gene sequencing results identified *Bacillus toyonensis* and *Bacillus thuringiensis* as the dominant genera in healthy larvae, while *Bacillus aryabhatai* and *Bacillus megaterium* were more prevalent in the diseased larvae. This study is the first to investigate the midgut microbiota of *A. proylei* from a biodiversity hotspot in northeastern India. Our findings may provide important insights into disease prognosis and management strategies for tasar silkworms, which are crucial for the local economy.

**Keywords:** Gut microbiota, *Antheraea proylei*, 16S rRNA, Tasar silkworm, Histopathology

**Received:** 06 February 2023

**Revised:** 28 April 2023

**Accepted:** 05 May 2023

**How to Cite This Article:** Devi YR, Lourebam DS, Modak R, Shantibala T, Subharani S, Rajashekar Y. Differences in Gut Microbiota of Healthy and Tiger Band Disease-Infected Oak Tasar Silkworms (*Antheraea proylei* J.). Entomol Lett. 2023;3(1):18-27.

<https://doi.org/10.51847/sReC3NTiUx>

### Introduction

The Northeastern region of India is known for its diverse range of wild silkworm species, making it a hub for wild silk production, including muga, oak tasar, mulberry silk, and eri [1]. Tasar silk has deep socio-cultural and traditional significance in India, playing a crucial role in the rural economy and contributing to the nation's agricultural and economic landscape [2]. One of the key species in this industry is the oak tasar silkworm, *Antheraea proylei* J., which is primarily farmed for tasar silk production in Manipur. This species results from the crossbreeding of the male Indian *A. proylei* and the female Chinese *A. pernyi* [3]. The quantity and quality of tasar silk depend on various factors, including environmental conditions, the health of the silkworm, and its ability to absorb nutrients. The physiology of the silkworm, particularly its digestion, growth, and immune system, is

influenced by the microbiota present in the midgut. Despite this, no silkworm breeds have been identified as entirely pests or resistant to diseases. At the larval stage, silk glands contribute to silk production, but infections affecting these glands can impair growth and result in significant economic losses [4]. Given that disease-infected silkworms are unable to produce cocoons, it is crucial to study the cytological damage in both the silk glands and the gut. Previous histopathological studies have shown that viruses, such as *Bombyx mori* nucleopolyhedrovirus (BmNPV), cause damage to internal tissues and silk glands during viral infections [5, 6]. Understanding the changes in gut microbiota during disease conditions can offer insights into the health and nutrition of silkworms [7] and help inform strategies to manage infections and improve their condition.

The gut microbiota plays a critical role in maintaining host health by regulating digestion, absorption, and nutrient assimilation [8]. It is also involved in the production of pheromones, degradation of pesticides, vitamin synthesis, and providing immunity against pathogens [9]. These bacteria protect the host by resisting invading microbes and enhancing the immune response [10]. Pathogenic microorganisms can infect all animal species, leading to diseases and even death, but the immune system provides protection [11]. Insects, especially their larvae, are more vulnerable to bacterial infections and the virulence factors of pathogens compared to vertebrates, which results in alterations to the host's defense mechanisms [12]. Laboratory-based culture studies on insect gut microbiota often fail to capture the full diversity of microbial species, as these methods only detect a limited number of dominant bacterial genera and cannot identify those with lower abundance [13]. Therefore, the use of the 16S rRNA gene as a molecular marker provides a more comprehensive view of bacterial diversity in insect gut microbiota [14]. The gut microbiota is undoubtedly integral to the health and nutrition of silkworms, highlighting the importance of further research in this area.

There is limited information available on the gut bacterial communities of various silkworm species, including *A. proylei*, in diseased conditions. The molecular profiling of the gut microbiota in this economically valuable silkworm has not been extensively studied, with only a few DNA sequences available [14-23]. Furthermore, there is a significant gap in our understanding of how pathogens, nutrient absorption, and disease development in silkworms affect their gut microbiota. Given this, research into the gut microbiota is crucial for understanding the microbial diversity linked to the production of silkworms. To date, there have been very few studies on the profiling and histopathological analysis of gut microflora in silkworms. This research wanted to compare the gut microbiota of *A. proylei* larvae in a healthy state and those infected with Tiger band disease during the fifth instar stage, all raised under controlled conditions, using 16S rRNA sequencing. Additionally, we examined histopathological alterations in the midgut and silk glands to assess the extent of tissue damage caused by the infection. Our research could provide valuable insights into disease management strategies, supporting the conservation of wild sericulture biodiversity for ecological stability and long-term economic sustainability.

## Materials and Methods

### Sample collection

In the summer of 2019, both healthy and Tiger band disease-infected fifth instar *A. proylei* larvae were collected from the Regional Sericulture Research Station, Mantripukhri, Manipur, with details provided in **Table 1** and **Figure 1**. Infected larvae were identified by the distinct black tiger-stripe pattern on their bodies, indicative of Tiger band disease [14]. To ensure sterile conditions, tools like forceps, scissors, and gloves were used during the collection process. Once collected, the larvae were kept in an ice-cooled box for transportation. Upon reaching the laboratory, the samples were disinfected by immersion in 70% ethanol and washed three times with sterile distilled water. Dissections to obtain midgut tissue and larvae were conducted in a sterile environment using dissection scissors. The intestinal contents were preserved in 50% glycerol at -80 °C for future research [16]. Three-fifths of the larvae were used for gut extraction and the bacteria within were isolated for further study. Following the isolation of the bacteria, the larvae were kept in a sterile environment at a controlled temperature of  $26 \pm 1$  °C and 70% relative humidity at the Animal Resources Division Laboratory, IBSD, Takyelpat, Manipur, India.

**Table 1.** Geographic information and collection sites of *A. proylei* from the regional sericulture research station, manipur (April–September 2019)

Collection description of oak tasar silkworm								
Locality	District	Instars	GPS coordinates	Altitude	Season	Temp. (°C)	RH (%)	Host Plant

Mantripukhri	Imphal West	4 <sup>th</sup>	N24°50'19.20" E093°56'34.78"	773	April 2019	18-30	70-90	<i>Quercus serrata</i>
Mantripukhri	Imphal West	4 <sup>th</sup>	N24°50'19.00'' E093°56'34.70''	772	June 2019	25-32	75-90	<i>Quercus serrata</i>
Mantripukhri	Imphal West	4 <sup>th</sup>	N24°50'19.20'' E093°56'34.77''	772	September 2019	25-34	75-90	<i>Quercus serrata</i>
Mantripukhri	Imphal West	4 <sup>th</sup>	N24°50'19.19'' E093°56'34.78''	773	June 2019	25-32	75-90	<i>Quercus serrata</i>
Mantripukhri	Imphal West	4 <sup>th</sup>	N24°50'19.21'' E093°56'34.68''	773	August 2019	25-34	75-90	<i>Quercus serrata</i>
Mantripukhri	Imphal West	4 <sup>th</sup>	N24°50'19.00'' E093°56'34.79''	773	June 2019	25-32	75-90	<i>Quercus serrata</i>

This table outlines the geographical conditions and specific locations where the fourth-stage *A. proylei* larvae were collected from the Regional Sericulture Research Station in Manipur during the period from April to September 2019, before being brought to the laboratory for further analysis.



**Figure 1.** Oak tasar silkworm larvae, *Antheraea proylei* J. a) healthy and, b) disease larva suffering from Tiger band disease.

#### *Isolation and cultivation of intestinal bacteria*

The guts of both healthy and infected *A. proylei* larvae were homogenized in a 0.86% NaCl solution. The resulting homogenates were serially diluted, plated in triplicate, and incubated for 24-48 hours at 37 °C. Bacterial colonies were identified based on their size, shape, and color, followed by further purification using successive streaking on agar plates. The purified bacterial strains were then cultured and stored in glycerol stocks for future use.

#### *Histopathological examination*

For histopathological analysis, both healthy and disease-infected fifth instar *A. proylei* larvae were collected from the Regional Sericulture Research Station, Mantripukhri, Manipur, India. Organs such as the silk glands and guts were dissected from both normal and Nucleopolyhedrovirus (NPV) infected silkworms. These tissues were preserved in a 10% formaldehyde solution and then fixed in Bouin's fluid. The tissues were dehydrated using alcohol and embedded in paraffin wax for sectioning. Sections of 5-7 µm thickness were stained with hematoxylin and eosin. Structural and histopathological changes were observed under a Leica DM 3000 LED microscope, and images were captured using a Leica DFC450 C camera.

#### *DNA extraction and 16S rRNA sequencing*

The DNA was extracted from the intestinal contents using the Gsure Bacterial Genomic DNA isolation kit, following the manufacturer's protocol. The DNA quality was assessed via agarose gel electrophoresis, and its concentration was measured using a Nanodrop spectrophotometer (Thermo Fisher Scientific). The DNA was then normalized to 200 ng/µL. Universal primers FD1 (5'-AGAGTTTGATCCTGGCTCAG-3') and RD1 (5'-AAGGAGGTGATCCAGCCGCA-3') were used to amplify the 16S rRNA gene. The PCR reaction was carried out in a 25 µL volume, containing 200 ng of DNA, 5X Phusion HF buffer, 10 mM of each dNTP, 2.5 U of Phusion DNA Polymerase, and 0.5 µM of forward and reverse primers.

The PCR cycle conditions were as follows: 94 °C for 5 minutes; 35 cycles of 94 °C for 1 minute, 50 °C for 30 seconds, 72 °C for 2 minutes, followed by a final extension at 72 °C for 10 minutes. The amplified PCR products were analyzed by 1% agarose gel electrophoresis and visualized using a Gel Documentation System (Bio-Rad). The products were purified using the GeneJET purification column and sequenced using a BigDye® terminator kit (Applied Biosystems Inc., Foster City, CA). The sequences were analyzed on an ABI 3500xL Genetic Analyzer (Eurofins Pvt Ltd, Bangalore, India) and aligned with GenBank sequences using the Blast search algorithm. The resulting sequences were submitted to GenBank, where they were assigned unique accession numbers.

### Sequence analysis

To assess sequence similarity, BLAST searches were conducted using the GenBank database. Sequence alignment was performed using the CLUSTALW tool within MEGA7 software. Phylogenetic analysis of proteolytic bacteria, based on the 16S rDNA gene, was utilized to explore the evolutionary relationships among the bacteria. The 16S rDNA sequences were used to search for reference nucleotide sequences in the NCBI GenBank database via the BlastN tool. The phylogenetic tree, representing the evolutionary relationships of the bacterial isolates, was constructed using the Neighbor-Joining method and the Kimura 2-parameter model. Bootstrap analysis with 1000 replications was conducted for each clade to assess the statistical significance of the tree.

## Results and Discussion

During the fifth instar stage, healthy larvae exhibit a strong feeding behavior, consuming leaves continuously and resting for short periods. They often seek fresh leaves even before finishing the previous ones, and their body color is light green. In contrast, infected larvae display noticeable symptoms, including reduced feeding and sluggish movement. The color of their integument fades, and the inter-segmental regions swell. Milky fluid begins to ooze from the anus, mouth, and body pores, indicating internal organ damage. As the infection progresses, the larvae's skin becomes thin and fragile, covered by a yellowish, amorphous substance with the formation of pores. Severely infected larvae cease feeding after molting, their bodies shrink, and they eventually turn black. Many of these larvae die during the spinning process, while a few survivors produce thin and weak cocoons.

In healthy silkworms, the 3 layers of the silk glands—tunica glandular layer, propria, and tunica intima—are visible. The secretory cells in these glands are packed with granules and are broader than the tunica propria. The nuclei of these cells are generally circular, and located on the basal lamina, which separates the secretory layer from the hemocoel. The tunica propria is narrow, and its lumen is filled with silk mass. The glandular zone contains numerous hemocytes with branched nuclei (**Figure 2a**).

In contrast, when the worms are infected, the silk gland's structure is compromised. The tunica propria loses its integrity, and the secretory layer becomes indistinguishable from it. The gland cells undergo rupture and damage, with the nuclei becoming enlarged and spindle-shaped, often filled with inclusion bodies. Vacuolization is also prominent. The lumen becomes distorted, and oil droplets can be seen suspended in the silk mass, which loses its density and compactness (**Figure 2b**).

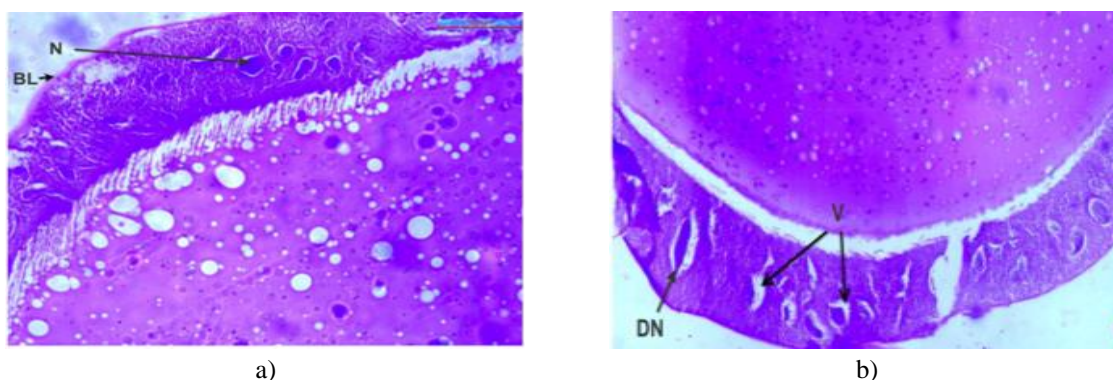


**Figure 2.** a) silk gland of a healthy silkworm, displaying intact tunica propria (TP) and abundant nuclei (N) (Bar = 100  $\mu$ m); and b) diseased silk gland exhibiting the loss of tunica propria (TP) integrity; at the advanced stage of infection, larvae show small, spherical nuclei (N) along with vacuole formations (V) (Bar = 100  $\mu$ m).

The midgut is the longest portion of the alimentary canal and consists of an outer muscle layer and an inner epithelial layer, which are separated by a basement membrane. In healthy silkworms, the histology of the midgut reveals an epithelial layer composed of enteric cells resting on the basement membrane. This is followed by an outer layer of longitudinal muscle cells and an inner layer of circular muscle cells. The epithelial layer is folded into villi, and the epithelial cells are categorized into 3 types: columnar, goblet (secretory), and regenerative cells. Columnar cells are tall, with granular cytoplasm, and are closely packed together. Their nuclei are large, spherical, or elliptical, and are located in the middle or upper half of the cell. Goblet cells, which are flask-shaped, have their nuclei positioned centrally, with most of the cytoplasm concentrated in the basal region, secreting mucus into the lumen. Regenerative cells, small and irregularly shaped, are located at the base of the epithelium and replace damaged epithelial cells during molting. These basal cells are situated between the columnar cells and the basement membrane (**Figure 3a**).

In the infected silkworms, the epithelial layer of the midgut loses its continuity. Histological slides from diseased larvae display distorted columnar cells with abnormal nuclei, massive vacuolization, scattered secretions, and a poorly defined basement membrane. Both goblet and columnar cells in the midgut show hypertrophy, with large vacuoles present. Absorptive cells appear completely overloaded, indicating a loss of their absorption capacity. The inter-cellular spaces widen, and individual cells become detached from the basement membrane. Nuclear changes include hypertrophy, pyknosis, and in some cases, anuclear cells. Regenerative, goblet, and basal cells are less evident in the infected larvae. Necrotic cell debris is dispersed within the lumen and hemocoel, and viral inclusion bodies are present in varying quantities within the cells. The midgut of the infected larvae is significantly damaged, resulting in a disorganized cellular arrangement. Furthermore, bacterial aggregates, appearing as dark masses, are visible inside the lumen, suggesting infection has breached the epithelial layer (**Figure 3b**).

The midgut's columnar cells secrete enzymatic granules involved in digestion and absorption, while goblet cells fulfill the secretory function. Regenerative cells divide to replace apoptotic cells, ensuring the continued function of the gut. The histological changes observed in this study align with those previously described in a study on passalid beetles [24]. By comparing the midgut of diseased silkworms and healthy, we gain a deeper understanding of the pathogenic effects that diseases can impose on tissues, cells, and organs. Since infected silkworms fail to spin cocoons, the analysis of cellular damage in the silk glands is critical. As the digestive system plays a vital role in defending against pathogenic microbes, our findings highlight the importance of studying this region. Beyond its digestive and absorptive functions, the midgut also acts as a barrier to invading pathogens. Our results show significant damage to the silk glands in infected larvae, with ruptured and deformed glands and the formation of lump cells, a stark contrast to the healthy larvae. This cytotoxic damage disrupts the silkworms' ability to maintain homeostasis.

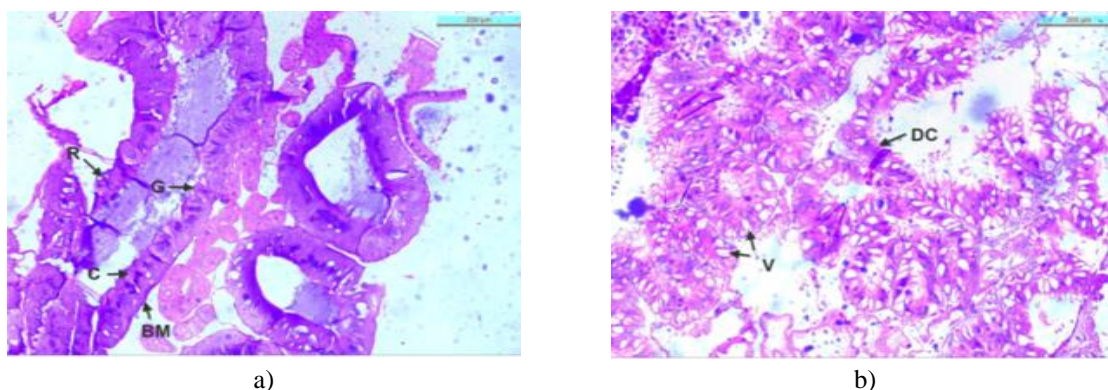


**Figure 3.** a) cross-sectional view of the midgut from healthy fifth instar larvae of *A. proylei*, showing columnar epithelial cells (CEC) and compact, darkly stained nuclei (N) (Bar = 200  $\mu$ m), b) cross-sectional view of the midgut from diseased fifth instar larvae of *A. proylei*, displaying hypertrophied columnar epithelial cells (CEC) and vacuoles (V) within the cytoplasm (Bar = 200  $\mu$ m).

Histopathological alterations in the midgut caused by viral infections and bacteria have been previously reported in other silkworm species [25-28]. In this study, the pathology associated with Tiger band disease appears to be primarily concentrated in the silk glands and midgut. Common pathological features observed in the infected larvae include nuclear hypertrophy, the presence of inclusion bodies in the cytoplasm, and vacuolization, which

ultimately lead to the death of the insects. These observations regarding midgut epithelial changes are consistent with findings from previous studies [29].

The infection is believed to initiate in the midgut, where it penetrates the basement membrane of the midgut wall and spreads to the hemocoel, infecting hemocytes, hypodermis, fat body, muscle, trachea, and silk glands. The highly alkaline gut environment, with a pH ranging from 9.5 to 11.5, along with possible enzymatic degradation, is thought to facilitate the breakdown of viral pathogens ingested by the silkworms [30].

The infection process begins with the endocytosis of viral particles from the diet, followed by viral replication and multiplication within the host cells, eventually leading to the release of new viral particles as the infected cells burst [31]. However, the silk gland presents an additional barrier: the extracellular fibrous matrix known as the basal lamina. The virus must penetrate this lamina to infect the gland. Recent studies suggest that the thickness and structural organization of the basal lamina act as a selective barrier, limiting the passage of macromolecules [6]. The tracheal system also plays a crucial role in spreading the infection from the hemocoel to the silk glands [32]. The trachea penetrates the basal lamina, allowing the virus to access the glandular epithelium, where it establishes a new replication cycle, as evidenced by nuclear enlargement and the formation of viral inclusion bodies.

We conducted a phylogenetic analysis to evaluate the similarity and classification of the 16S rRNA sequences from both unidentified and identified bacterial strains using distance-based neighbor-joining methods in MEGA 6 and sequence similarity searches via the BLAST program. The sequence analysis revealed that most of the gut bacterial isolates exhibited a 99% similarity. The 16S rRNA sequences of these isolates were deposited in GenBank under accession numbers MT416410.1 to MT416415.1, and the details are summarized in **Table 2**.

**Table 2.** Details of 16S rRNA gene sequence of gut bacteria isolate from *A. proylei* in this study.

Sl No.	Sample ID of tasar silkworm	Organism with the closest match from GenBank	Site of collection	GenBank accession No.	Similarity
1	N_H02	<i>Bacillus toyonensis</i>	Mantripukhri	MT416410.1	99.55%
2	D_C03	<i>Bacillus aryabhatai</i>	Mantripukhri	MT416411.1	99.89%
3	D_D03	<i>Bacillus aryabhatai</i>	Mantripukhri	MT416412.1	99.55%
4	D_E03	<i>Bacillus aryabhatai</i>	Mantripukhri	MT416413.1	99.66%
5	D_F03	<i>Bacillus aryabhatai</i>	Mantripukhri	MT416414.1	98.99%
6	D_G03	<i>Bacillus aryabhatai</i>	Mantripukhri	MT416415.1	99.77%

The 16S ribosomal RNA gene sequences were compared using the BLAST (basic local alignment search tool) method. The sample IDs correspond to various gut bacteria isolated from the oak tasar silkworm, showing the highest similarity (98-100%) with their closest matches in the GenBank database. The sequences were submitted to GenBank, with assigned accession numbers ranging from MT416410.1 to MT416415.1.

Analysis of the 16S rRNA gene sequences from *A. proylei* revealed that *Firmicutes* dominate the bacterial composition, with the genus *Bacillus* being the most prevalent, representing ten different species. The family Bacillaceae was notably abundant in the guts of both infected and healthy *A. proylei* larvae, as outlined in **Table 3**. Our study indicates that *Bacillus* is the primary genus identified from the laboratory cultures of gut bacteria in *A. proylei*.

**Table 3.** Taxonomic profile of gut bacterial isolates of *A. proylei* identified by 16S rRNA gene sequences

Samples	Group	Family	Genus	Species
Healthy silkworm	Firmicutes	Bacillaceae	Bacillus	<i>Bacillus toyonensis</i>
				<i>Bacillus thuringiensis</i>
				<i>Bacillus pacificus</i>
				<i>Bacillus mobilis</i>
				<i>Bacillus mycoides</i>
Disease silkworm	Firmicutes	Bacillaceae	Bacillus	<i>Bacillus megaterium</i>
				<i>Bacillus aryabhatai</i>
				<i>Bacillus zanthoxyli</i>
				<i>Bacillus flexus</i>
				<i>Bacillus simplex</i>

Phylogenetic analysis of the gut microflora from both healthy and diseased tasar silkworms revealed a 6% difference between the two groups. Evolutionary phylogenetic distances were calculated using the maximum composite likelihood method [33]. To better understand the evolutionary relationships of the intestinal bacteria, a phylogenetic tree was constructed (Figure 4) based on the 16S rRNA sequences, employing the neighbor-joining method with 1000 bootstrap replications.

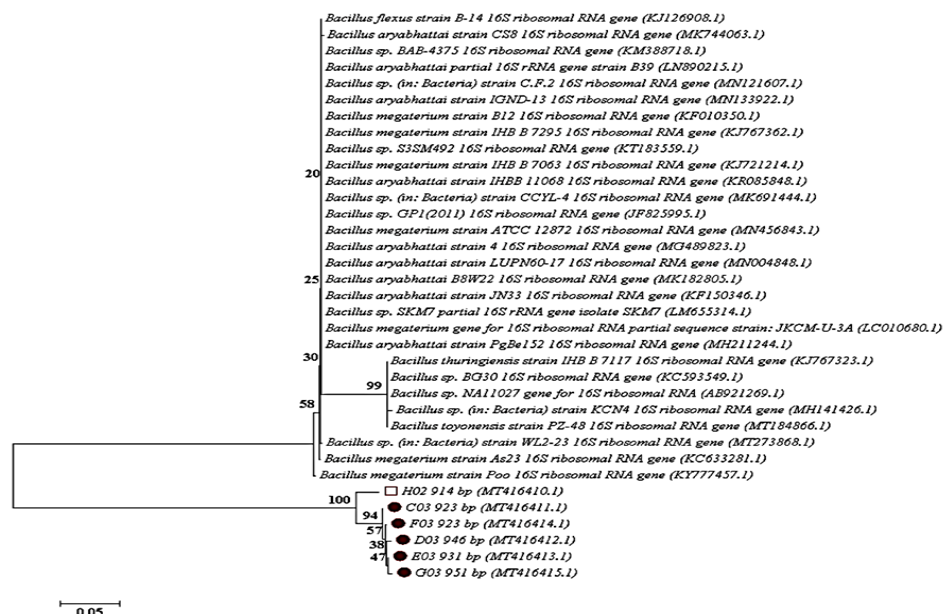


Figure 4. Phylogenetic tree of gut bacteria isolated from the gut of *Antheraea proylei*

In diseased silkworms, *Bacillus aryabhatai* appears to be the most prevalent genus across all affected individuals. In contrast, healthy silkworms predominantly harbor microflora like *B. toyonensis* and *B. thuringiensis*, which share a high sequence similarity, showing more than 99% identity with sequences found in the GenBank database. *Bacillus* species are commonly used in agriculture as biopesticides and biofertilizers [34] and as potential probiotics for both humans and animals [35-37]. Therefore, our findings may contribute to exploring the potential application of *Bacillus* species against various pathogenic gut microflora. Silkworms, along with other Lepidopteran insects, have long been valuable both culturally and economically. A diverse range of bacterial species, from obligate endosymbionts to facultative ones, inhabit the gut microflora of most insects [38].

Further research into the bacterial diversity and its interactions with the insect host, particularly from various geographical regions, will provide a deeper understanding of their crucial roles in insect health and disease. While some limited information on the gut flora of the tasar silkworm, *A. proylei*, from the Northeastern regions of India exists, it remains inconclusive. This study used a 16S rRNA gene sequence-based approach to examine the gut bacterial communities associated with *A. proylei* populations in Manipur, Northeastern India.

Our findings reveal that the tasar silkworm harbors a distinctive gut microbiota, with Firmicutes being the dominant phylum and *Bacillus* the predominant genus, making up nearly 100% of the total gut bacterial isolates in *A. proylei*. Similar studies have shown that the gut of the gypsy moth (*L. dispar*), a Lepidopteran species, is predominantly populated by *Pseudomonas* and *Bacillus* species [4]. The results from this study align with research on the gut bacterial diversity in *Bombyx mandarina* and *Bombyx mori*, where Firmicutes was identified as the dominant bacterial phylum through 16S rRNA gene sequencing [39]. *Bacillus* has also been shown to be the most abundant bacterial genus, constituting nearly 18% of the gut flora in 21 different insect species, as documented in earlier studies [40]. A 16S rRNA gene analysis of *P. xylostella* larvae's gut bacteria also revealed limited bacterial diversity [41]. Similarly, our phylogenetic analysis of tasar silkworm gut bacteria showed a relatively low diversity in bacterial phylogenetic groups.

Our analysis identified Firmicutes as the dominant family, forming a prominent clade, with *Bacillus* as the main genus, including ten distinct species (Figure 4). Further molecular phylogenetic analysis confirmed that Firmicutes and *Bacillus* are the predominant clade and genus in both healthy and diseased silkworms. A more in-

depth investigation from diverse regions within Northeastern India would help enhance our understanding of the gut microbiota's diversity and composition in oak tasar silkworms, as well as its role in disease management.

Diseased larvae are a major source of potential viral outbreaks in silkworm populations [42]. Due to the high virulence, the pathogenicity of the virus is sustained in deceased larvae, which can continue to spread the infection in silkworm-rearing rooms. Therefore, it is crucial to carefully remove these larvae, ensuring their skin remains intact and undisturbed to prevent further transmission.

The variations in the characteristics of nucleopolyhedrovirus infections are influenced by several factors, such as the virulence of the viral strain, the quantity of ingested viral particles, the stage of larval development, co-infection with other pathogens, and optimal rearing conditions, including temperature, population density, and food availability [32, 42]. As the virus replicates in the fat body tissues of the infected larvae, food reserves are depleted, hindering the development of the silkworm's organs. The adults that emerge from these infected cocoons often show deformities, reduced activity, and compromised health. The debilitating effects of viral diseases in Lepidoptera include developmental delays, reduced adult weights and pupal, decreased silk production, and ultimately a decline in overall silk yield.

## Conclusion

This study represents one of the initial efforts to genetically and histopathologically characterize the midgut microbiota of *A. proylei* found in Manipur, a region in northeastern India. To gain a deeper understanding of how microbiota influences immunity, nutrition, and reproduction in this key silkworm species, a more detailed and expansive investigation of midgut bacteria is essential. Our research not only sheds light on the progressive degradation of the *A. proylei* larvae's midgut but also clarifies the level of damage caused by infections, which subsequently affects the silk glands. Additionally, exploring the probiotic potential of the gut microflora remains a key challenge. The insights gained from this study could significantly enhance our knowledge of disease resistance mechanisms and the management of *A. proylei* silkworm populations.

**Acknowledgments:** None

**Conflict of Interest:** None

**Financial Support:** None

**Ethics Statement:** None

## References

1. Lokeshwari RK, Shantibala T. A review on the fascinating world of insect resources: reason for thoughts. *Psyche*. 2010;2010(0033-2615). doi:10.1155/2010/207570
2. Reddy RM. Conservation need of tropical tasar silk insect, *Antheraea mylitta* Drury (Lepidoptera: Saturniidae)-strategies and impact. *J Entomol*. 2010;7(3):152-9.
3. Jolly M. Inter-specific hybridization in *Antheraea*. *Indian Heredity*. 1969;1:45-8.
4. Brancalhão R, Torquato E, Fernandez M. Cytopathology of *Bombyx mori* (Lepidoptera: Bombycidae) silk gland caused by multiple nucleopolyhedrovirus. *Genet Mol Res*. 2009;8(1):162-72.
5. Khurad A, Mahulikar A, Rathod M, Rai M. Infection of nucleopolyhedrovirus in the larval rudiments of gonads of silkworm, *Bombyx mori* L. *Indian J Seri*. 2005;44(2):159-64.
6. Zhu F, Li D, Song D, Huo S, Ma S, Lü P, et al. Glycoproteome in silkworm *Bombyx mori* and alteration by BmCPV infection. *J Proteom*. 2020;222:103802. doi:10.1016/j.jprot.2020.103802
7. Dee Tan IY, Bautista MAM. Bacterial survey in the guts of domestic silkworms, *Bombyx mori* L. *Insects*. 2022;13(1):100. doi:10.3390/insects13010100
8. Zhang X, Zhang F, Lu X. Diversity and functional roles of the gut microbiota in lepidopteran insects. *Microorganisms*. 2022;10(6):1234.
9. Jaffar S, Ahmad S, Lu Y. Contribution of insect gut microbiota and their associated enzymes in insect physiology and biodegradation of pesticides. *Front Microbiol*. 2022;13:979383.

10. Chen K, Lu Z. Immune responses to bacterial and fungal infections in the silkworm, *Bombyx mori*. *Dev Comp Immunol*. 2018;83:3-11. doi:10.1016/j.dci.2017.12.024
11. Miyashita A, Kizaki H, Kawasaki K, Sekimizu K, Kaito C. Primed immune responses to gram-negative peptidoglycans confer infection resistance in silkworms. *J Biol Chem*. 2014;289(20):14412-21.
12. Waterfield NR, Daborn PJ, French-Constant RH. Insect pathogenicity islands in the insect pathogenic bacterium *Photorhabdus*. *Physiol Entomol*. 2004;29(3):240-50.
13. MsangoSoko K, Gandotra S, Chandel RK, Sharma K, Ramakrishnan B, Subramanian S. Composition and diversity of gut bacteria associated with the eri silk moth, *Samia ricini*, (Lepidoptera: Saturniidae) as revealed by culture-dependent and metagenomics analysis. *J Microbiol Biotechnol*. 2020;30(9):1367-78. doi:10.4014/jmb.2002.02055
14. Shantibala T, Devi KM, Lokeshwari RK, Anju S, Luikham R. Complete mitochondrial genome of a latent wild oak tasar silkworm, *Antheraea frithi* (Lepidoptera: Saturniidae). *Mitochondrial DNA Part B*. 2018;3(1):15-6.
15. Yang J, Zhang RS, Chen DB, Chen MM, Li YP, Liu YQ. The complete mitochondrial genome of *Antheraea proylei* strain In981 (Lepidoptera: Saturniidae). *Mitochondrial DNA Part B*. 2019;4(2):2264-5.
16. Shantibala T, Fraser MJ, Luikham R, Devi Y, Devi K, Lokeshwari RK, et al. Genetic characterization of an alphabaculovirus causing tiger band disease in the oak tasar silkworm, *Antheraea proylei* J. (Lepidoptera: Saturniidae). *Sericologia*. 2018;58:91-111.
17. Broderick NA, Raffa KF, Goodman RM, Handelsman J. Census of the bacterial community of the gypsy moth larval midgut by using culturing and culture-independent methods. *Appl Environ Microbiol*. 2004;70(1):293-300.
18. Weisburg WG, Barns SM, Pelletier DA, Lane DJ. 16S ribosomal DNA amplification for phylogenetic study. *J Bacteriol*. 1991;173(2):697-703.
19. Altschul SF, Madden TL, Schäffer AA, Zhang J, Zhang Z, Miller W, et al. Gapped BLAST and PSI-BLAST: a new generation of protein database search programs. *Nucleic Acids Res*. 1997;25(17):3389-402.
20. Kumar S, Stecher G, Tamura K. MEGA7: molecular evolutionary genetics analysis version 7.0 for bigger datasets. *Mol Biol Evol*. 2016;33(7):1870-4.
21. Saitou N, Nei M. The neighbor-joining method: a new method for reconstructing phylogenetic trees. *Mol Biol Evol*. 1987;4(4):406-25.
22. Kimura M. A simple method for estimating evolutionary rates of base substitutions through comparative studies of nucleotide sequences. *J Mol Evol*. 1980;16(2):111-20.
23. Tamura K, Nei M, Kumar S. Prospects for inferring very large phylogenies by using the neighbor-joining method. *Proc Natl Acad Sci*. 2004;101(30):11030-5.
24. Reyes-Castillo P. Coleoptera, Passalidae: morfología y división en grandes grupos; géneros americanos. *Coleoptera, passalidae: morphology and division into large groups; American genera. Folia Entomol Mex*. 1970;20:217-32.
25. Choudhury A, Guha A, Yadav A, Kumari J, Unni BG, Roy MK. Induced immunity in *Antheraea assama* Ww larvae against flacherie causing *Pseudomonas aeruginosa* AC-3. *Exp Parasitol*. 2004;106(3-4):75-84.
26. Jurat-Fuentes JL, Jackson TA. Bacterial entomopathogens. In *Insect Pathol*. 2012;2:265-349.
27. Mohanta MK, Saha AK, Saleh DK, Islam MS, Mannan KS, Fakruddin M. Characterization of *Klebsiella granulomatis* pathogenic to silkworm, *Bombyx mori* L. *3 Biotech*. 2015;5(4):577-83. doi:10.1007/s13205-014-0255-4
28. Ponnuvel KM, Nakazawa H, Furukawa S, Asaoka A, Ishibashi J, Tanaka H, et al. A lipase isolated from the silkworm *Bombyx mori* shows antiviral activity against nucleopolyhedrovirus. *J Virol*. 2003;77(19):10725-9. doi:10.1128/jvi.77.19.10725-10729.2003
29. Khurad AM, Mahulikar A, Rathod MK, Rai MM, Kanginakurdu S, Nagaraju J. Vertical transmission of nuclear polyhedrovirus in the silkworm, *Bombyx mori* L. *J Invertebr Pathol*. 2004;87(1):8-15.
30. Tinsley TW, Harrap KA. Viruses of invertebrates in comprehensive virology, In: Fraenkel-Conrat H, Wagner RR, eds. *Comprehensive Virology*. Vol. 12. New York: Plenum Publishing Corp; 1978; p. 1-101.
31. Herniou EA, Olszewski JA, Cory JS, O'Reilly DR. The genome sequence and evolution of baculoviruses. *Annu Rev Entomol*. 2003;48(1):211-34.
32. Torquato EF, Neto MH, Brancalhão RM. Nucleopolyhedrovirus infected central nervous system cells of *Bombyx mori* (L.) (Lepidoptera: Bombycidae). *Neotrop Entomol*. 2006;35(1):70-4.

33. Felsenstein J. Confidence-limits on phylogenies—an approach using the bootstrap. *Evolution*. 1985;39(4):783-91. doi:10.2307/2408678
34. Dame ZT, Rahman M, Islam T. Bacilli as sources of agrobiotechnology: recent advances and future directions. *Green Chem Lett Rev*. 2021;14(2):246-71. doi:10.1080/17518253.2021.1905080
35. Lee NK, Kim WS, Paik HD. Bacillus strains as human probiotics: characterization, safety, microbiome, and probiotic carrier. *Food Sci Biotechnol*. 2019;28(5):1297-305. doi:10.1007/s10068-019-00691-9
36. Luise D, Bosi P, Raff L, Amatucci L, Viridis S, Trevisi P. Bacillus spp. probiotic Strains as a potential tool for limiting the use of antibiotics, and improving the growth and health of pigs and chickens. *Front Microbiol*. 2022;13:801827. doi:10.3389/fmicb.2022.801827
37. Elshagabee FM, Rokana N, Gulhane RD, Sharma C, Panwar H. Bacillus as potential probiotics: status, concerns, and future perspectives. *Front Microbiol*. 2017;8:1490.
38. Dillon RJ, Dillon V. The gut bacteria of insects: nonpathogenic interactions. *Annu Rev Entomol*. 2004;49(1):71-92.
39. Kumar D, Sun Z, Cao G, Xue R, Hu X, Gong C. Study of gut bacterial diversity of Bombyx mandarina and Bombyx mori through 16S rRNA gene sequencing. *J Asia-Pac Entomol*. 2019;22(2):522-30.
40. Yun JH, Roh SW, Whon TW, Jung MJ, Kim MS, Park DS, et al. Insect gut bacterial diversity determined by environmental habitat, diet, developmental stage, and phylogeny of host. *Appl Environ Microbiol*. 2014;80(17):5254-64.
41. Indiragandhi P, Anandham R, Madhaiyan M, Poonguzhali S, Kim GH, Saravanan VS, et al. Cultivable bacteria associated with larval gut of prothiofos-resistant, prothiofos-susceptible and field-caught populations of diamondback moth, Plutella xylostella and their potential for, antagonism towards entomopathogenic fungi and host insect nutrition. *J Appl Microbiol*. 2007;103(6):2664-75. doi:10.1111/j.1365-2672.2007.03506.x
42. Adams JR, McClintock JT. Baculoviridae. Nuclear polyhedrosis viruses. Part 1. Nuclear polyhedrosis viruses of insects. In: Adams JR, Bonami JR, eds. Atlas of invertebrate viruses. Florida: CRC Press; 1991. p. 89-180.